

Author response ACP manuscript egusphere-2026-479

The comments of the reviewers are written in black.

The response of the authors is given in blue with the general answer to the comment in roman. *Changes in the manuscript are presented in italics, where unchanged lines are also blue, but edited and newly added paragraphs are given in orange.*

General comments

As required by the editorial support, we exchanged the red colouring in Tabs. 1 and 2 to bold font. Furthermore, we removed the grey colouring in Tab. 2 and simply refer to it by the brackets. Please also note that we updated the affiliations of two authors.

After a discussion with Alberto de Lozar during the time of the revision, we adapted the discussion section to take into account that the simulated case in de Lozar and Mellado (2017) is in fact, a thick case, even though the simulated case is the same as in Bretherton et al. (2007) and Pistor and Mellado (2025). The confusion originated from the specific setup of the DNS used in de Lozar and Mellado (2017). This does not change any results or conclusions presented in the paper. We added the following sentence and adjusted some more details accordingly (see the tracked changes manuscript for all the changes).

We identify this as the main difference from the simulations of Bretherton et al. (2007) and Pistor and Mellado (2025), both of which simulated active droplet sedimentation for 6 h. Their case from the first research flight (RF01) of the Second Dynamics and Chemistry of Marine Stratocumulus (DYCOMS-II) field campaign (Stevens et al., 2005) also belongs to the thin category with a LWP of around 40 g m^{-2} . Note here that due to the specific setup, the DNS study of de Lozar and Mellado (2017) does not belong to the thin, but the thick category, even though they also took DYCOMS-II RF01 as a reference case (A. de Lozar, 2026, pers. comm.). As for Bretherton et al. (2007) and Pistor and Mellado (2025),

Response to reviewer 1

General Comment

This paper addresses a less explored issue of the impact of cloud water sedimentation on the stratocumulus to cumulus transition at its early stages. The topic is relevant, the goal of the paper is well-defined, the methodology used is mostly valid, and the results are interesting. The writing is already of good quality. I recommend publishing the paper after major revision.

We thank the reviewer for their valuable comments, which have helped to improve our manuscript. Please find our responses below.

Specific comments

Please clarify that the saturated and unsaturated cases relate to optically thick and thin clouds, as the current terms can easily be confused with saturated and unsaturated air. I suggest considering a change in terminology to “optically thick” and “optically thin” clouds

We agree with the reviewer that the previous notation was not clear enough. Thus, we accepted the suggestion and renamed “saturated” to “optically thick” (or simply “thick”) and “unsaturated” to “optically thin” (or simply “thin”) throughout the manuscript. As this is a general edit, we refer to the tracked changes manuscript for details.

Introduction:

The process-level explanation of what happens during the SCT, including the impact of the diurnal cycle, is also provided in van der Dussen (2014) and Kurowski et al. (2025). An important recent observational study of Pugsley et al. (2025) highlights the role of nighttime processes on aerosol-cloud interactions, whereas Lebsock et al. (2024) show the response of LWP to aerosol perturbations.

Thank you for providing these valuable articles, we included the studies of van der Dussen (2014) and Kurowski et al. (2025) in the introduction when discussing the diurnal cycle. However, we prefer not to mention aerosol-cloud interactions there directly, as this is not the focus of our study. That said, we agree with the importance of these studies, so we added them to the new paragraph in the discussion section, where we discuss our findings in the context of the study by Glassmeier et al. (2021) regarding time scales (see the response to reviewer #2). Please find our altered introduction below.

Increased entrainment together with overshooting cumuli eventually leads to the dissipation of the stratocumulus deck and its replacement by shallow cumuli (Bretherton and Wyant, 1997; Wyant et al., 1997). It has further been demonstrated recently that the diurnal cycle is profoundly impacting the SCT, as the coupling of the boundary layer to the moisture supply differs between day-time and night-time conditions. While the stratocumulus deck is mostly coupled to the moisture supply at night, either directly or through the mixed layer cumuli, solar insolation drives decoupling throughout the day (van der Dussen et al., 2013; Kurowski et al., 2025).

While the dynamical mechanism is widely accepted, it has been shown in recent years that the SCT is also influenced by microphysically induced processes like precipitation.

Section 2.1

It suggests a 1-D approach (SCM); Please clarify.

We agree that this is confusing, so we shortened the paragraph to the relevant information:

In this study, we conduct idealised large-eddy simulations (LES) using the Icosahedral Nonhydrostatic (ICON) model (Zängl et al., 2015; Dipankar et al., 2015). To enable periodic boundary conditions, the simulations are run on a planar torus grid, which automatically connects the respective boundaries.

McGibbon and Bretherton showed that LES can be used to mimic observations on a moving platform (ship), with important changes in the mean thermodynamic state accounted for via advective tendencies. However, your approach assumes continuity of cloud-related processes as if it were a Lagrangian mass-conserving perspective. What is the relevance of your approach to a Lagrangian one if you do not adjust for the impact of microphysical changes? Furthermore, depending on the ship’s speed, the impact of cloud water sedimentation will be different in this setup, which is not physical.

We thank the reviewer for raising this important point. It is true that our approach is not fully Lagrangian, as we are in the ship-following frame of reference. The ship moves at 10 m s^{-1} southwest through the SCT. This is faster than the mean winds of our 10 cases, which vary between $4 - 7 \text{ m s}^{-1}$ and faster than mean trajectory speeds of 7 m s^{-1} in Eastman and Wood (2016). The orientation of the ship’s movement is largely aligned. To account for this inaccuracy we performed additional sensitivity experiments, where we mimic a slower moving air mass by halving the update frequency of our large-scale forcing input. I.e. the large-scale forcing applied at time t_0 is now prescribed for times t_0 and t_1 , while the original large-scale forcing at time t_1 is now prescribed at times t_2 and t_3 , and so on. For this idealised slower moving air mass, we repeat our *control* and *drop_sed* experiments for both Leg 16A (thick) and Leg 04A (thin).

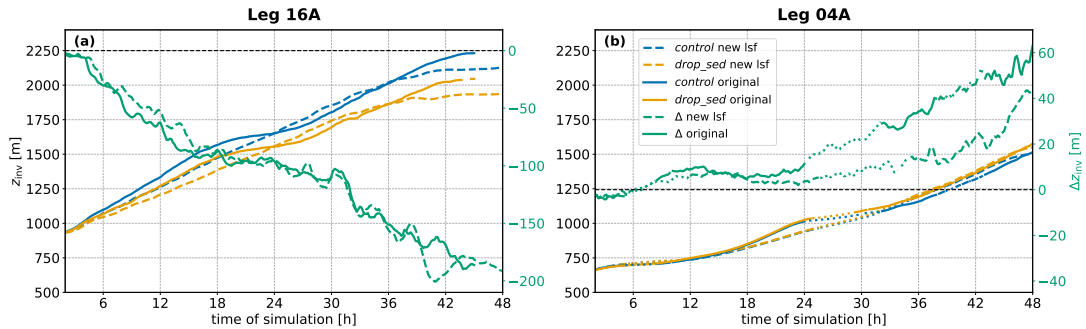


Figure 1: Inversion height of (a) Leg 16A and (b) Leg 04A with the original runs in solid and the new large-scale forcing (lsf) experiment in dashed. To include as many data points as possible, a reduced spinup window of 2 h is removed from the simulations. Dotted lines in panel (b) represent intermittent periods, where the cloud fraction falls below 40%.

The result is presented in Fig. 1 with an optically thick leg in panel (a) and a thin one in panel (b). While the adjusted forcing simulations of the thick case deepen at different rates (as expected) in contrast to the ship-following simulations, the difference induced by droplet sedimentation (green lines) remains virtually unchanged. For the thin case, the findings are more nuanced. The mechanism is qualitatively not impacted. An ini-

tial entrainment reduction is followed by an increase in entrainment, which dominates the response over longer time scales. However, quantitatively the results differ, as the quicker deepening in the ship-following forcing simulations in itself increases LWP and thus cloud-top longwave cooling. We thus see a compound effect in the diverging green lines, which is however fully consistent with the mechanisms presented here.

As we feel that this should be clarified to the readership of the manuscript, we added the following to Sect. 2.1.

It should be noted, that this ship-following setup is not truly Lagrangian. With an average speed of 10 m s^{-1} , the ship moves faster than the mean wind speed of 6.9 m s^{-1} identified in Lagrangian SCT trajectories (Eastman and Wood, 2016). This was explored in sensitivity experiments (not shown), which used a reduced (halved) update frequency of the large-scale forcing mimicking a slower-moving idealised trajectory. Our results were not qualitatively affected, and our conclusions remain unchanged.

What is the configuration of the control run? Is it simply without cloud water sedimentation?

Yes that is the only difference, thanks for pointing that out. We added this to the original statement:

We simulate one control run (control) and one run with active droplet sedimentation parametrisation (drop_sed) for each leg for 48 h in an 8 km by 8 km domain with 50 m horizontal resolution. Hereby, the drop_sed configuration is identical to the control configuration, with the only difference being the activation of cloud droplet sedimentation in the ICON microphysics directly from the start of the simulation.

When you run your simulations for 6 hours to spin up the model, do you account for any diurnal cycle during that phase? It seems to be a high-impact approach during which the model already develops significant differences between the control and other simulated states. What exactly happens during that phase in terms of the mean cloud state and droplet number concentrations? What is the purpose of it? Does it lead to significantly different initial states? Does it change the response of the WTG correction? It needs to be clarified, because all the differences you get at later times may strongly depend on that initial state.

We did not suppress the diurnal cycle during spinup and indeed the composite analysis of the thick cases includes averaging across different times of day. This was unavoidable to show this difference between two distinct regimes. To be clear, spinup in our study simply refers to the initial period of the simulation, which we cut in the analysis to avoid including artifacts of model spinup into our analysis. There is no "spinup stage", in which all simulations are forced with a constant large-scale forcing, but we directly start with the ship-following forcing of each leg, respectively, and also directly activate droplet sedimentation in the *drop_sed* experiments from the beginning (the only exception here is the spinup experiment for Leg 04A, see below). On top of that, we think that the different starting times in between legs are an advantage in our setup, as we can show this way that the initial reduction in entrainment occurs independent of the starting time (cf. Tab. 2). Furthermore, this important observation also remains intact for an individual leg at different activation times of droplet sedimentation. This can be observed in the spinup experiment for the optically thin Leg 04A. While the main *drop_sed* simulation started in the late morning (local time), sedimentation in the spinup experiment was activated during the late night (local time). Table 2 shows that, while the initial reduction

in entrainment obviously differs quantitatively, it occurs in both cases independent of the time of day. Nuances with respect to the diurnal cycle sensitivity will be assessed in a follow-on study of this.

Regarding the concern of spinup and potential different representations of initial states, we can assure the reviewer that this is not the case. As can be seen in Fig. 1 shown in the previous comment (which shows the most of the spinup time explicitly), the simulations do not strongly diverge during this spinup phase. We believe the confusion may have come from Fig. 6, which has been revised since. The figure did not show simulation results after 6h of spinup, but rather from the last 14 hours of the 40h simulation. Thus the majority of the response had already occurred, and differences are not attributable to a difference in spinup. This difference made more explicit (see our response to the comment on Fig. 6). So as shown in Fig. 3 of the manuscript and Fig. 1 in the responses, we have very similar initial states from which our sensitivity experiments start. For a detailed response on the WTG correction, we would like to refer the reviewer to our response to your comment on Sect. 2.3, where the same concern is raised.

Furthermore, your Fig. A4 shows that you indeed start with significantly different initial states: 100 g/m² vs 200 g/m², which immediately impacts further cloud development. Yes, that is true, but this is because these are two inherently different types of simulations: While the solid lines are the default, precipitating runs, the dashed lines represent simulations where we artificially disabled precipitation formation. It is expected that for the precipitating Leg 16A, this leads to a much stronger cloud deck with much more liquid water.

However, the crucial point here is also that droplet sedimentation is activated from the beginning. This means, even if we cut the spinup for the analysis, *control* and *drop-sed* start from the same initial state and there is no bias introduced through different initial states. It is true that there is a rather large difference between solid and dashed in Fig. A4, but the important differences between the respective *control* and *drop-sed* simulations (the colouring) are small. Lastly it can be noted that, although the LWP difference is more than double, the qualitative course of Δz_{inv} is the same during the first night (cf. Fig. 10 in the manuscript), i.e. the deviations between the respective *control* and *drop-sed* are comparable, independent of the overall cloud state.

Section 2.2

L113: “low” relative to what?

We meant “low” relative to the other hydrometeors, as rain, snow or graupel. In usual vertical mesh sizes of several tens of meters, the settling movement of cloud droplets is negligible, as they need roughly $t = 70 \text{ m} / 3 \text{ cm s}^{-1} \approx 40 \text{ min}$ to reach the next grid box for $dz = 70 \text{ m}$ and a sedimentation velocity of 3 cm s^{-1} . For our case, this reduces by a factor of $70/9$ leading to $\approx 5 \text{ min}$. We clarified this as follows:

The original ICON two-moment microphysics scheme does not contain the process of sedimenting cloud droplets due to their low sedimentation velocity of a few cm s^{-1} , compared to other hydrometeors like rain, snow or graupel that can reach up to 10 m s^{-1} (Pruppacher and Klett, 1997).

L114: What do you want to say in this sentence? It is unclear.

We wanted to note that even though the process of cloud droplet sedimentation is not

included in the ICON two-moment scheme, it can be added in a numerically convenient fashion, as the structure of spherical hydrometeor sedimentation is already present in terms of e.g. ice. Thus, only the cloud droplet related coefficients for the gamma distribution as well as the corresponding routines need to be added in an analogous way. That being said, we agree that this sentence is confusing and does not add valuable information here, so we removed it.

L119-125: Explain all the symbols used. What are N , L , m here? This paragraph needs more clarification.

We apologise for the confusion, we wanted to keep this paragraph concise, but this also made it harder to follow. We now refined it and added more explanations:

Hydrometeor masses x are assumed to follow the generalised Γ -distribution

$$f(x) = A x^\nu \exp(-\lambda x^\mu), \quad (1)$$

with the hydrometeor-specific shape parameters μ, ν and the coefficients

$$A = \frac{\mu M_0}{\Gamma(\frac{\nu+1}{\mu})} \lambda^{\frac{\nu+1}{\mu}} \quad \text{and} \quad \lambda = \left[\frac{\Gamma(\frac{\nu+1}{\mu}) M_1}{\Gamma(\frac{\nu+2}{\mu}) M_0} \right]^{-\mu}. \quad (2)$$

The latter depend on the first two moments M_m of the distribution, which can be obtained by evaluating

$$M_m = \int_0^\infty x^m f(x) dx \quad (3)$$

for $m = \{0, 1\}$. Since $f(x)$ describes the hydrometeor size distribution, the $m = 0$ integration over the whole size spectrum yields the number density N of the respective hydrometeor species, i.e. $M_0 := N$. Analogously, the first moment is written as the mass density L of the respective hydrometeor species, i.e. $M_1 := L$.

Note: For cloud droplets specifically, this implies that $N = N_d$ and $L = q_c$ if we adapt the notation followed in this manuscript.

In a two-moment scheme, both initial moments N and L are predicted. Sedimentation is addressed by solving the partial differential equation

$$\frac{\partial M_m}{\partial t} = -\frac{\partial}{\partial z} (\bar{v}_m \cdot M_m) \quad (4)$$

with the mean sedimentation velocity \bar{v}_m of each moment $m = \{N, L\}$ and species individually. \bar{v}_m itself can be obtained by computing the respective velocity-weighted moment

$$\bar{v}_m = \frac{1}{M_m} \int_0^\infty v(x) x^m f(x) dx \quad (5)$$

using the sedimentation velocity $v(x)$ of each hydrometeor species.

This section lacks comparison of cloud droplet sedimentation to Bretherton et al. (2007). What is similar? What is different? Are the values of terminal velocity comparable between their study and yours?

We agree, there are indeed some noteworthy differences. For brevity, we write SB06 for Seifert and Beheng (2006), which is the scheme used in this study and B07 for Bretherton et al. (2007). Firstly, while SB06 assume a generalised Γ -distribution for the hydrometeor masses (cf. Eq. (1)), B07 assume that cloud water follows a lognormal radius (r) distribution. For the terminal fall velocity, both approaches describe it via a Stokes velocity, but SB06 also introduce a density correction $\sim \rho^{-0.2}$ to account for the change in atmospheric density with height. Secondly, B07 prescribes cloud droplet number concentration as a constant value of $N_d = 140 \text{ cm}^{-3}$, whereas in the two-moment scheme of SB06, N_d is prognostic, so it varies over the course of the transect.

To compare the absolute values of the terminal velocity, one can transform the velocity-mass relation

$$v(x) \simeq \alpha x^\beta \left(\frac{\rho_0}{\rho} \right)^\gamma \iff v(r) = \alpha \left(\frac{2r}{a} \right)^{\beta/b} \left(\frac{\rho_0}{\rho} \right)^\gamma \quad (6)$$

(cf. Eq. (6) of the revised manuscript) to a velocity-radius relation using the diameter mass relation $D(x) = 2r(x) = ax^b$ from Eq. (32) of SB06, where a and b are again hydrometeor-specific constants. Plugging in the correct numbers for cloud droplets ($a = 0.124 \text{ m kg}^{-\beta}$, $b = 1/3$, $\alpha = 3.75 \cdot 10^5 \text{ m s}^{-1} \text{ kg}^{-\beta}$, $\beta = 2/3$, implying $\beta/b = 2$) and assuming an air density of $\rho = 1.110 \text{ kg m}^{-3}$ yields $v(r) = c_{\text{SB}} r^2$ with $c_{\text{SB}} \approx 1.0 \cdot 10^8 \text{ m}^{-1} \text{ s}^{-1}$ for the present work. The formula of B07 is of the same structure with a factor of $c_{\text{B}} = 1.19 \cdot 10^8 \text{ m}^{-1} \text{ s}^{-1}$, implying that B07 assume a 19% larger sedimentation velocity. Note here that we corrected a typo in the coefficient α in the manuscript. We added the following to Sect. 2.2:

The present formulation features two key differences from Bretherton et al. (2007). Firstly, while Seifert and Beheng (2006) assume a generalised Γ -distribution for the hydrometeor masses (cf. Eq. (1)), Bretherton et al. (2007) assume that cloud water follows a lognormal radius (r) distribution. For the terminal fall velocity, both approaches describe it via a Stokes velocity, but Seifert and Beheng (2006) also introduce a density correction $\sim \rho^{-\gamma}$ to account for the change in atmospheric density with height. Secondly, in the study of Bretherton et al. (2007), cloud droplet number concentration is prescribed at a constant value of $N_d = 140 \text{ cm}^{-3}$, that fits to their case study. In the two-moment microphysics of the present study, N_d is prognostic, so it varies over the course of the transect.

Transforming the velocity-mass relation from Eq. (6) to a velocity-radius relation using the diameter $D(x) = ax^b$ yields the same Stokes terminal velocity as reported by Bretherton et al (2007):

$$v(r) = \frac{4\alpha}{a^2} \left(\frac{\rho_0}{\rho} \right)^\gamma r^2 \equiv cr^2. \quad (7)$$

Inserting $a = 0.124 \text{ m kg}^{-\beta}$ and $b = 1/3$ for cloud droplets and an air density of $\rho = 1.110 \text{ kg m}^{-3}$ yields $c \approx 1.0 \cdot 10^8 \text{ m}^{-1} \text{ s}^{-1}$ in the present study. Comparing this to the value $c = 1.19 \cdot 10^8 \text{ m}^{-1} \text{ s}^{-1}$ from Bretherton et al. (2007) reveals a deviation of about 19%, implying that the fall velocity in the latter is slightly higher than in this setup.

Section 2.3

It seems that the WTG corrections can strongly alter the simulated state and can also be simulation-dependent. Is that the case? If yes, wouldn't it be more reasonable to turn them off completely and focus on studying the subtle effects of cloud water sedimentation without them? When comparing two different simulation results, does it mean you are

looking at both cloud water sedimentation and different WTG effects combined? If yes, then how do you attribute the differences to cloud water sedimentation only?

Thanks for addressing that, this is a crucial point. We agree that a WTG correction during the simulation (as done originally by McGibbon and Bretherton, 2017) would distort the interpretation of the cloud water sedimentation impact. That is why we employ an 'offline' approach here, prior to all the experiments. We first compute the WTG correction in a prior set of simulations for each leg separately and apply the same correction to all scientific experiments. The strategy is as follows (individually for each leg):

- 1) We interpolate the original large-scale forcings from McGibbon and Bretherton (2017) to fit to the ICON grid (let's call them *lsf_no_wtg*).
- 2) We conduct *control* runs (i.e. no droplet sedimentation) for all legs on a coarser grid using *lsf_no_wtg* (let's call the output *no_wtg*), but do not apply the WTG correction during the runs.
- 3) We use the full finished output *no_wtg* to compute the WTG correction *w_wtg_1* to the base forcing vertical velocity *w_lsf_no_wtg* afterwards. We add these together at all timesteps and acquire *lsf_wtg_1* with *w_lsf_wtg_1*.
- 4) We now go back to step 2) and perform a set of *control* runs *wtg_1* with the new forcings *lsf_wtg_1*.
- 5) Then we repeat step 3) with *wtg_1* to compute a second iteration of the WTG correction *w_wtg_2*, that is added to *w_lsf_wtg_1* in *lsf_wtg_2*. This is required in some cases, since the offline application can lead to overcorrections in the later stages, as it does not take into account the changes from previous time step.
- 6) Lastly, we conduct another set of *control* runs *wtg_2* with these forcings *lsf_wtg_2*.
- 7) We then compare *wtg_1* and *wtg_2* for each leg to the observed inversion height and decide on the optimal configuration of the large-scale forcings (i.e. *lsf_wtg_1* or *lsf_wtg_2*). This large-scale forcing configuration is then **fixed** (see column six of Tab. 1) and used for the main runs of **both** *control* and *drop_sed*.

This way, cloud droplet sedimentation is directly responsible for the observed effects between *control* and *drop_sed*.

We extended Sect. 2.3 to clarify the above approach as follows (note that in the manuscript the names as *no_wtg* are written in italics):

In the setup of McGibbon and Bretherton (2017), this correction was calculated during the simulations to adjust the vertical velocity dynamically. We cannot adopt this procedure in our study, since we want to compare the outcome of control and drop_sed targeting the cloud droplet sedimentation mechanism. Applying a dynamical correction would distort the sedimentation effect, as in both cases the simulations would be drawn to the reference profiles. To nevertheless obtain results, that qualitatively fit to the observations, we opt for an offline WTG correction.

Before performing the main runs that are presented in this study, we conduct control runs no_wtg for each leg with the original large-scale forcings based on McGibbon and Bretherton (2017)(called lsf_no_wtg), but without an application of the WTG correction during the runs. We do this in a low resolution setup on a 4km by 4km domain with around 132m horizontal resolution. Moreover, we only use 200 vertical levels with a layer thickness of at most 25m below 3km and stretched above. Lastly, we strictly nudge the simulation state to the reference temperature and humidity above 3km on a time scale of 1min to ensure that reference and simulation are correctly synced above the boundary layer. Note that this coarser setup produces results that are qualitatively similar to those obtained at finer resolution.

Using the `no_wtg` outputs, we compute the WTG correction offline for all time steps based on Eq. (9), add it to the original vertical velocity from the large-scale forcings and obtain new large-scale forcings `lsf_wtg_1`. Using the latter, we perform first iteration control runs `wtg_1`, completely identical to before, but with the adapted vertical velocity. Clearly, this approach will not work flawlessly, as changes from previous time steps are not taken into account this way and thus, overcorrections can occur in the later stages. To account for this, we repeat our procedure and compute the offline WTG correction for the `wtg_1` runs, thus obtaining `lsf_wtg_2`. Using this, we perform second iteration runs `wtg_2`, compare them to `wtg_1` and choose the best fit iteration for the forcings (i.e. `lsf_wtg_1` or `lsf_wtg_2`) for each leg based on the development of the inversion height. This (leg-dependent) forcing configuration is fixed and serves as input for the main runs of both control and `drop_sed`, respectively. The individual choices for the iterations can be found in Table 1. This approach yields a consistent outcome for all cases, exhibiting the characteristic deepening and the sub-cloud layer cumulus evolution, which is the main point of interest in our study (cf. Fig. A1).

Furthermore, we added the following to Sect. 2.1 in order to clarify the origin of our large-scale forcings.

The simulations are initialised using the first applicable ship-launched sounding and forced using geostrophic winds, ship-following advective tendencies for temperature and humidity and the large-scale vertical velocity. These forcings were adapted for ICON based on the original ones from McGibbon and Bretherton (2017).

Section 3.1

Do your calculations of pseudo-albedo account for solar zenith angle? Kurowski et al. (2025) show how to include it.

We thank the reviewer for pointing that out. Our calculations did not include solar zenith angle and we updated both Fig. 2 and the numbers in the discussion using the approach presented in Kurowski et al. (2025). For the latter, we excluded all solar zenith angles exceeding 80° from the analysis, as the Sun is then located close to the horizon. All in all, there were no qualitative, but only quantitative changes (see the tracked changes document). We further updated Sect. 3.1 as follows:

The small embedded rectangle shows the LES pseudo-albedo A of the 8 km by 8 km domain at the time of satellite snapshot, which serves as a proxy for the real albedo. We adopt the approach outlined in Kurowski et al. (2025) based on Meador and Weaver (1980) to include the solar zenith angle. Note that while Fig. 2 only displays a snapshot, we will briefly address the albedo susceptibility in the discussion, where we excluded angles $> 80^\circ$ when the sun is located near the horizon. A is computed as

$$A = (1 - f_c) \alpha_{\text{sfc}} + f_c A_c, \quad (8)$$

with the ocean albedo $\alpha_{\text{sfc}} = 0.06$ and the cloudy albedo A_c . The latter is computed using the individual albedo of a cloudy layer α_{cld} (Stephens, 1984):

$$A_c = \alpha_{\text{cld}} + \frac{\alpha_{\text{sfc}} (1 - \alpha_{\text{cld}})^2}{1 - \alpha_{\text{sfc}} \alpha_{\text{cld}}}. \quad (9)$$

Furthermore, we calculate the optical depth τ for α_{clid} using the approach of Stephens (1978):

$$\tau = \sum_{i=c,r} \frac{3}{2} \int \frac{q_i(z) \rho(z)}{r_{\text{eff},i}(z) \rho_w} dz, \quad (10)$$

summing over the individual contributions of cloud and rain water. ρ represents the local air density, $\rho_w = 1000 \text{ kg m}^{-3}$ represents the density of water, r_{eff} and q denote the effective radius and the mixing ratio of the respective liquid hydrometeor. For the sake of brevity, we refer to Appendix A of Kurowski et al. (2025) for the details of the computation of α_{clid} .

When comparing cloud albedo, did you use GOES-15 effective radius? How does it compare to the LES? Running LES on an $8 \text{ km} \times 8 \text{ km}$ domain has strong limitations on the maximum size of cloud structures represented in the domain. Such small domains are not feasible for simulating changes in closed vs open cell dynamics, which needs to be clarified. Can you provide any numbers regarding cloud albedo values from LES and GOES? I assume they are compared at the same local times.

While GOES-15 data is usually not post-processed to yield quantities like albedo directly, additional post-processing was performed for the period of the MAGIC campaign (i.e. 01 Oct. 2012 to 30 Sep. 2013) to provide more comprehensive data to compare with the ship observations. This was done by Patrick Minnis' group at NASA/Langley using the VISST algorithm (originally developed for the CERES instrument, but calibrated for geostationary satellites), described in Minnis et al. (2011). Thus, we directly used the albedo included in this product. We did not compare the effective radii, as this would require the usage of a satellite simulator, which is not available for GOES for ICON. This is why we only show albedo, which can be compared with pseudo-albedo calculations from the LES directly for spherical droplets. We agree with the reviewer, that any form of mesoscale organisation is not adequately captured on such small domains. Thus, the visualisation was used for qualitative purposes only and our analysis restricted to the pre-breakup stage, since the stratiform stage can be simulated reasonably well (e.g. Bretherton et al., 2007, McGibbon and Bretherton, 2017).

We updated this section to clarify this:

The magnitude of the pseudo-albedo largely matches the satellite in both cases. Similarly, both simulation domains capture the qualitative differences in cloud morphology between the two cases described above. The thick Leg 16A case exhibits a broad cloud deck covering most of the LES domain, whereas Leg 11A is far less extensive and features more isolated cumuli, consistent with conditions in the breakup region. In both cases peak albedos inside individual cumuli exceed observed albedo ranges. Furthermore, the simulated cloud deck during Leg 16A seems to be a little more broken than observed. However, it is important to be aware of the scales. The LES domain corresponds to only two by two pixels in the satellite image, which thus (by design) cannot capture any scales of mesoscale organisation. Overall, it is encouraging that the individual simulations exhibit analogous differences to those shown in the satellite images.

L48: This comparison is rather qualitative given all the differences mentioned above. Yes, we agree. Given the limitations of domain size, we cannot make meaningful quantitative comparisons, as mesoscale organisation is missing (see previous comment).

Figs 4 and 5: How does this comparison change for different times of day and night? Do the differences depend on it?

The reviewer raises an interesting question here, but in this manuscript we wanted to focus on systematic changes associated with droplet sedimentation. We expect that disentangling the impacts during day- and night-time would likely induce more individual effects, of which the detailed analysis is beyond the scope of this study. That said, since this is an active area of research at the time being, we intend to investigate diurnal cycle effects in the context of the SCT in a future project.

Fig. 6: The two evolutions shown are almost the same but shifted in the vertical because of the differences in the initial state. Consequently, the differences between the two oscillate around that initial difference. That figure shows that the 48 h evolution is not much different, but the initial spin-up leads to the main differences. How big of a contribution comes from WTG corrections? Are they assumed to be the same in both cases shown?

We realise that we did not provide sufficient detail in the caption and had potentially misleading axis labels. Regarding the WTG correction, we would like to refer you to our response to your comment in Sect. 2.3, where this has now been clarified in the manuscript. We acknowledge that the labelling the x-axis of Fig. 6 with UTC was not a good choice, as this does not indicate in any way how much time has passed in this particular Leg 12A simulation. We exchanged this with the distance from LA on the bottom, so it is now comparable to Fig. 3, panel (a) and added the information of the shown time window in the caption. We hope this clarifies the main point of this section, summarised below.

Figure 6 covers the hours 26 to 40 of Leg 12A (note that this transect starts around 1077 km from LA), so it is clear that the cloud state around 2100 km strongly depends on the time-integrated response to active droplet sedimentation, which explains the vertical shift of the inversion height z_{inv} from the beginning of the plot in panel (a). However, the key point is the difference in boundary layer growth speed (i.e the entrainment velocity, indicated by the slope of the green curve) in the displayed time window. The slope in the window of interest (marked by vertical dashed lines) is positive, even though this case was classified as thick in the beginning. The explanation for this can be found in panel (b), where the water paths are depicted. Day-time thinning through solar insolation lead to a thin cloud deck with LWPs below 50 g m^{-2} and almost no RWP. This is the deciding factor and key message of the figure, as longwave cooling is now no longer saturated (and the stabilising effect through precipitation is missing). During this time, an excess in LWP in *drop_sed* generated by droplet sedimentation away from the cloud top, drives temporarily increased LW cooling. With that, the turbulence feedback mechanism in the sedimentation case comes into play (more liquid water, more cooling, and more turbulence) that leads to the stronger entrainment generating the positive slope in panel (a). This point has also been clarified in the manuscript at the end of Sect. 4.1:

Furthermore, this demonstrates that the categorisation into optically thick and optically thin is not rigid. Especially initially thick legs can become thin over the course of one diurnal cycle, when solar insolation dries out the cloud deck during the day (as we saw here for Leg 12A), highlighting the importance of the diurnal cycle in the context of the SCT.

Do surface fluxes change between the control and other simulations? Does cloud water sedimentation have any impact on it?

The surface fluxes are computed using a simplified version of the Louis (1979) parametrisation, adapted for ICON. Hereby, the sensible heat flux is primarily determined by the difference between lowest model layer temperature and sea surface temperature (SST), where the latter is prescribed. The latent heat flux is primarily determined by the difference between lowest model layer specific humidity and sea surface humidity, where the latter is computed using the SST and the surface pressure. Additionally, other surface quantities as wind speed or density enter the parametrisation. This means, while the prescribed SST is the same in *control* and *drop_sed*, the fluxes themselves are not, as they depend on the lowest model layer quantities. Thus, cloud water sedimentation influences the surface fluxes, but only indirectly through the induced changes that eventually alter e.g. lowest model layer humidity or lowest model layer temperature.

As can be seen from Fig. 2 (heat fluxes representative cases, Leg 11A on the left, Leg 16A on the right), this leads to mostly minor changes for the optically thin cases, but to notable differences for the thick cases. The main reason is that precipitation evaporation near the surface is a major driver of the surface layer temperature and humidity, which only comes into play in the very end of Leg 11A (cf. Fig. 3, panel (d)) in the manuscript.

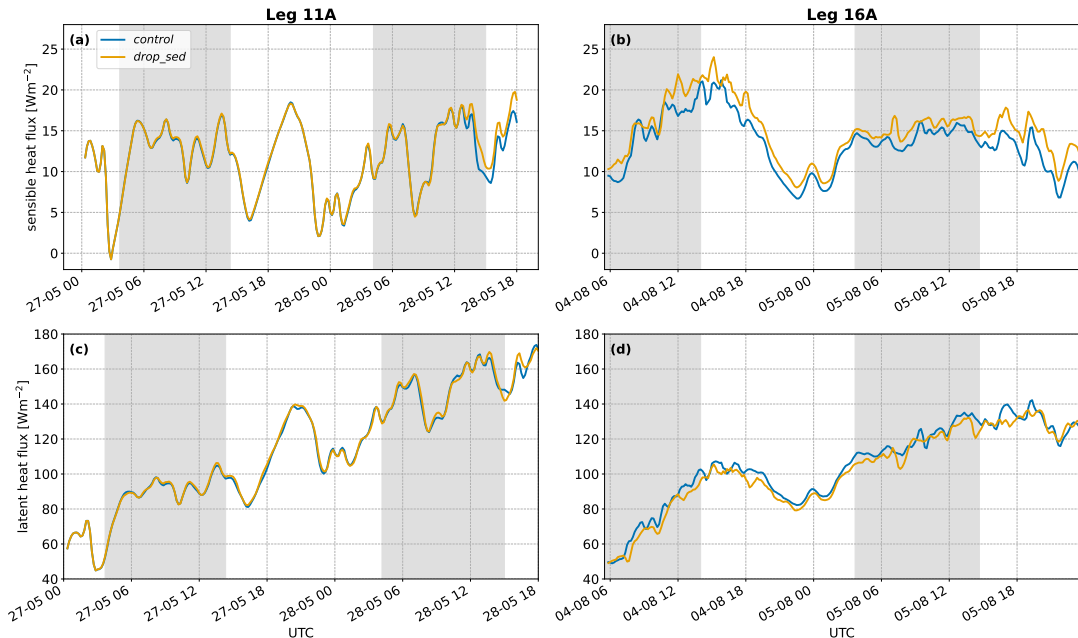


Figure 2: **Top:** Sensible heat fluxes of (a) Leg 11A and (b) Leg 16A. **Bottom:** Latent heat fluxes of (c) Leg 11A and (d) Leg 16A.

Have you looked at the differences in decoupling caused by sedimentation?

Yes, we have looked at decoupling induced by sedimentation by means of the humidity criterion introduced by Jones et al. (2011), however, we found the direct impact to be rather small. We computed the average humidity difference Δq_v between the lower and upper 25% of the boundary layer for all legs and compared the respective *control* and *drop_sed*. The result can be found in Fig. 3. We also added a horizontal line at $\Delta q_v = 1.5 \text{ g kg}^{-1}$, which is the appropriate decoupling threshold for MAGIC according to Zhou et al. (2015). Overall, the decoupling strengthens further away from the coast, in alignment with the course of the SCT. Focusing on the thick legs (all but 04A and 11A), *drop_sed* is always less decoupled than *control* in the later stages of the simulations, while

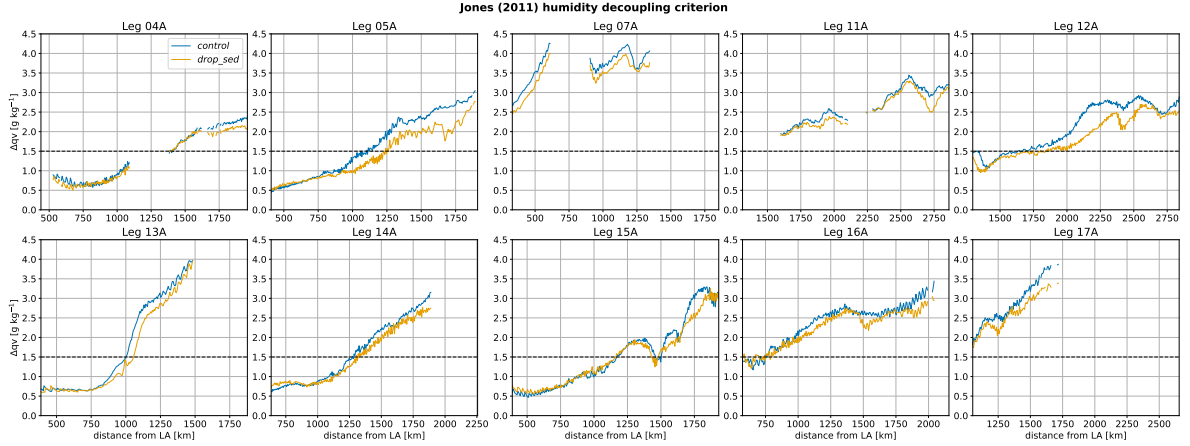


Figure 3: Average humidity difference Δq_v between the lower and upper 25% of the boundary layer.

it is roughly the same (or even slightly inverted) in the beginning. In the thin Leg 04A, there seems to be no real difference in decoupling apart from the end, while Leg 11A is also rather similar, until decoupling decreases in *drop_sed* at the end of the simulation. Recalling that all thick legs show stronger precipitation in *drop_sed*, we interpret this decoupling as an indirect consequence of cloud droplet sedimentation. Rain formation is increased, which stabilises the cloud and decreases entrainment, which in turn delays the decoupling of the boundary layer. In Leg 04A, where rain only starts to form very late and never reaches the surface, both *control* and *drop_sed* are in a similar (de-)coupled state, implying the direct impact of sedimentation on decoupling is small. Only in the end, when rain water forms (more efficiently in *drop_sed*), leaves the cloud and evaporates, *drop_sed* is less decoupled than *control*. This finding also aligns with Kurowski et al. (2025), who report for their precipitating case that decoupling is delayed in the presence of cloud water sedimentation.

Most statistics are reported using domain-averaged LWP, but radiative impacts and entrainment feedbacks are more directly tied to in-cloud properties (LWP_c weighted by cloud fraction, optical thickness τ_c). Please consider adding parallel in-cloud/conditional analyses (or at least a decomposition into cloud-fraction and in-cloud components) to better connect the results to satellite observables and recent ACI studies.

We thank the reviewer for pointing that out. We agree and consequently updated all reported LWP variables (tables and figures) by weighting the domain-averaged LWP by the corresponding area cloud fraction. Regarding the analysis, nothing changed qualitatively but only quantitatively, so we simply replaced the numbers and figures and stated that we now use the in-cloud liquid water path. For simplicity, we stuck with the notation LWP. We added the following in Sect. 2.4.

However, at lower values, this emissivity increases with LWP and so does the radiative cooling that drives stratocumulus development. In the following, LWP denotes the in-cloud liquid water path, which is computed by weighting the domain-averaged liquid water path by the corresponding area cloud fraction. As summarised in the last two columns of Table 1, eight legs fall in the thick category, while two belong to thin

The effects of cloud water sedimentation are also discussed in Kurowski et al. (2025),

in addition to the diurnal cycle analysis of cloud susceptibility to aerosols. How do your results compare to theirs? Part of the conclusions seem to be consistent with their sensitivity study. How does your process-level understanding relate to theirs?

The sensitivity experiment of Kurowski et al. (2025) is only indirectly comparable to our study, as they alter the cloud droplet number concentration N_d for a particular process, i.e. they use a higher (polluted) N_d for cloud droplet sedimentation, but keep N_d at the lower (pristine) baseline otherwise. Keeping that in mind, we can discuss the induced mechanisms that are independent of this.

The primary result of their sensitivity experiment is, that using the polluted N_d for droplet sedimentation leads to reduced rain water path and increased boundary layer growth compared to the pristine experiment. Sedimentation with higher N_d compared to lower N_d basically implies a reduction in sedimentation speed due to the smaller and more numerous droplets. Thus, we can roughly equate this experiment with our *control* runs without sedimentation and use the pristine case as the *drop_sed* runs of the optically thick cases due to the high RWP in Kurowski et al. (2025) (even though the LWP is mostly low, but we found the rain to be dominating over the longwave cooling, e.g. in the end of the thin Leg 11A). In that regard, our findings align with theirs, as we also find that enabling cloud droplet sedimentation leads to enhanced precipitation formation as well as reduced boundary layer growth. Furthermore, we agree with their interpretation that the removal of cloud water from the entrainment zone is driving the increase in precipitation production. We added the following to the discussion in the manuscript:

Kurowski et al. (2025) also investigated the impact of cloud water sedimentation in a sensitivity experiment. While they did not directly study disabled sedimentation versus enabled sedimentation, they conducted a low sedimentation versus high sedimentation experiment in a precipitating case (i.e. comparable to our thick cases). They found that stronger sedimentation leads to a reduction in entrainment together with an increase in rain water, which aligns well with our findings in the optically thick category. We also observe increased precipitation rates as well as reduced boundary layer growth in our simulations, when comparing drop_sed to control (cf. Fig. 3, panels a) and c)).

References:

Kurowski, M. J., Lebsock, M. D., and Smalley, K. M.: The diurnal susceptibility of subtropical clouds to aerosols, *Atmos. Chem. Phys.*, 25, 15329–15342, <https://doi.org/10.5194/acp-25-15329-2025>, 2025.

van der Dussen, J. J. and Co-authors (2013), The GASS/EUCLIPSE model intercomparison of the stratocumulus transition as observed during ASTEX: LES results, *J. Adv. Model. Earth Syst.*, 5, 483–499, doi:10.1002/jame.20033.

Pugsley, E., Gryspeerd, & V. Nair, Cloud fraction response to aerosol driven by nighttime processes, *Proc. Natl. Acad. Sci. U.S.A.* 122 (47) e2509949122, <https://doi.org/10.1073/pnas.2509949122> (2025).

Smalley, K. M., Lebsock, M. D., & Eastman, R. (2024). Diurnal patterns in the observed cloud liquid water path response to droplet number perturbations. *Geophysical Research Letters*, 51, e2023GL107323. <https://doi.org/10.1029/2023GL107323>

Jones, C. R., Bretherton, C. S., & D. Leon (2011): Coupled vs. decoupled boundary layers in VOCALS-REx, *Atmos. Chem. Phys.*, 11, 7143–7153, DOI: 10.5194/acp-11-7143-2011, <https://acp.copernicus.org/articles/11/7143/2011/>

Eastman, R., & R. Wood, 2016: Factors Controlling Low-Cloud Evolution over the Eastern Subtropical Oceans: A Lagrangian Perspective Using the A-Train Satellites. *J. Atmos. Sci.*, 73, 331–351, <https://doi.org/10.1175/JAS-D-15-0193.1>.

Response to reviewer 2

Review of “Opposing entrainment effects of cloud droplet sedimentation during the pre-breakup stage of the stratocumulus to cumulus transition” by Schnellke et al. (egusphere-2026-479) This study analyzes aerosol-cloud interactions during stratocumulus-to-cumulus transitions over the northeast Pacific using high-resolution numerical simulations. The authors show that adjustments in cloud water can be negative or positive, with clouds containing higher amounts of cloud water showing the former behavior and those containing lower amounts the latter. Overall, the addressed topic is important, the simulation results align with the current understanding of the topic, and the writing is good. However, the most important finding is not new, as I lay out in more detail below. Thus, I cannot recommend publishing this work.

We thank the reviewer for their time and review. However, there seems to be a misunderstanding here. While the findings of our work are applicable in their interpretation to adjustments generated by aerosol-cloud interactions, such as the one proposed in Bretherton et al. (2007), this paper does not assess “aerosol-cloud interactions during stratocumulus-to-cumulus transitions” as mentioned above. Indeed, we did not mention the term “aerosol-cloud interactions” in the original manuscript. Bretherton et al. (2007) propose that increases in droplet number concentration driven by aerosol perturbations, may alter cloud top entrainment rates by decreased cloud droplet sedimentation. This may impact the liquid water path (LWP) adjustment and is widely known in the community as the sedimentation-entrainment feedback, which may act in tandem with the entrainment feedback (Wang et al., 2003). This is also the only time that this study mentions the “LWP adjustment” (L666 original manuscript) and it is mentioned in this context only. This statement is then further embedded in a single short paragraph where the applicability of our findings to albedo susceptibility is mentioned although it is not “the primary focus of this study”, which is explicitly stated at the beginning of the paragraph (L661 original manuscript).

An alternative singular cloud condensation nuclei (CCN) concentration scenario in Sect. 4.3 is only considered to make sure that our findings in the thin LWP regime are not subject to incorrect background CCN concentrations. As further mentioned in the manuscript, the assumed background CCN concentration of 250 cm^{-3} “exceeds the acceptable range” for this optically thin case (L522-523 original manuscript). Thus, we test if our conclusions regarding mechanisms driven by *droplet sedimentation* remain valid.

We argue that it is stated with sufficient clarity in the abstract and introduction that this paper assesses the impact of *droplet sedimentation* on stratocumuli prior to cloud breakup along the stratocumulus to cumulus transition. Our work shows (for the first time) that the impact of *droplet sedimentation* depends on the time scale over which it is assessed and the background state (i.e. LWP) of the cloud and is **not** uniform. Therein lies the novelty of this study. There are interesting connections to the below mentioned studies, which are now explicitly mentioned in the manuscript. This is further discussed below.

Major Comment

Glassmeier et al. (2021) and Hoffmann et al. (2020) also showed that there are two types of liquid water adjustments: clouds with low amounts of cloud water tend to experience positive cloud water adjustments due to longwave radiative cooling exceeding losses in

cloud water by entrainment, while clouds with high amounts of cloud water tend to experience negative cloud water adjustments due to entrainment exceeding cooling. These previous findings are in strong agreement with the schematic shown in Fig. 11. Thus, the current study does not provide substantially new insights. Since Glassmeier et al. (2021) and Hoffmann et al. (2020) did not focus on stratocumulus-to-cumulus transitions, one could extend the current study to provide substantial new insights.

Glassmeier et al. (2021) show that the negative LWP adjustment in non-precipitating clouds cannot be fully captured in ship tracks, as these features do not live sufficiently long for the full negative LWP adjustment to manifest. For fixed external cloud controlling parameters all simulations conducted in the N_d -LWP phase space approach an equilibrium LWP (Fig. S1 of their manuscript). As stated in Glassmeier et al. (2021), increases in LWP from the initial low LWP state towards the equilibrium are driven by longwave cooling and decreases in LWP towards the equilibrium by entrainment for non-precipitating nocturnal stratocumulus decks for which most of the 144 simulations were conducted.

We do not dispute the key finding of this work (that when perturbed the system will relax over time to the equilibrium state), nor its importance for understanding aerosol-cloud interactions, but its applicability to our findings. Gravitational settling cannot be considered as a singular perturbation, setting a new initial condition from which the system relaxes back to its equilibrium state. This is implied by the reviewer by equating our findings to adjustment mechanisms from initialised low-LWP and high-LWP states to the fixed response line. Instead, we state that gravitational settling of droplets leads to temporally non-uniform interactions (short-term vs long-term response) with other regulating processes such as entrainment and longwave cooling under non-precipitating or weakly drizzling conditions. These statements are distinct and non-equivalent. The equilibrium line in Fig. S1A of Glassmeier et al. (2021) shows an equilibrium line forced by external parameters (divergence rates, surface fluxes, background aerosol concentration). The reviewer equates our mechanisms to the fact that the LWP will relax down to the equilibrium line (or surface in a higher-dimensional space) from a low- or high-LWP state. This is not the case. Our low and high LWP states have nothing to do with that equilibrium state line in Fig. S1A. Each of these cases has different external parameters, so each case has a different equilibrium line in the displayed N_d -LWP space. What our findings would actually imply if transferred to Glassmeier et al. (2021) is, that including droplet sedimentation may alter the path (and thus the slopes) of the evolution of their simulations through the N_d -LWP phase space if simulations with or without droplet sedimentation were contrasted. However, this phase space was never opened here, as the susceptibility to aerosol concentrations was never assessed.

The discussions of our findings in the context of Glassmeier et al (2021) is of interest, as it raises the issue of time scales. In the idealised simulations of Glassmeier et al. (2021), the process time scale (τ_{proc}), which in the context of LWP (or inversion height) adjustments is $\mathcal{O}(10 \text{ h})$, is convoluted with the time scale of changing external parameters, i.e. meteorological conditions (τ_{met}). The implications of this was widely discussed in Feingold et al. (2025). Since our simulations are not truly Lagrangian (from the perspective of the cloud), but ship-following we conducted idealised simulations of an altered τ_{met} (see the comment regarding Sect. 2.3 from reviewer #1). These simulations show, that quantitatively, the covariability of these time scales leads to quantitative differences, but not qualitative differences in the mechanistic process interactions. Even though $\tau_{\text{proc}} > \tau_{\text{met}}$ in our case, the interaction between the three processes considered (i.e. droplet sedi-

mentation, longwave cooling, and entrainment) remains qualitatively the same as LWP stays low (or high) and the system is only weakly precipitating. It is important to once again highlight, that the deciding threshold distinguishing between high- and low-LWP state process interactions, has nothing to do with the equilibrium LWP surface set by external parameters of Glassmeier et al. (2021), but the transition of the cloud from a radiatively transmissive to a radiatively opaque state.

Glassmeier et al. (2021) is based on the same set of simulations previously analysed in Hoffmann et al. (2020). The latter disentangle (together with mixed layer theory) the individual impacts of surface fluxes, entrainment, radiation, precipitation and cloud-top motion on the LWP- N_d state space. They concur with Glassmeier et al. (2021) that radiative cooling as well as entrainment are the dominant contributions. Using the mixed layer theory, they diagnose an analytical expression for this steady state and derive conditions for the stability of the latter by means of an entrainment velocity. The steady state LWP is found to vary depending on large-scale subsidence rates and/or surface fluxes between $10 - 80 \text{ g m}^{-2}$. The lower range would be in the thin, and the latter in the thick category of our study.

We do not dispute their findings. However, our argument is - as with Glassmeier et al. (2021), that our findings suggest droplet sedimentation could impact the speed at which they are reached. The speed here matters, as the time scale of the adjustment and the time scale of meteorological change (i.e. time scale of changing external parameters) covary (which is neglected in both studies), which can impact the net response along a perturbed cloud trajectory. Goren et al. (2025) even argue that the LWP change along the trajectory is entirely driven by changing external parameters, rather than cloud-scale adjustments.

It should also be noted, that Glassmeier et al. (2021) and Hoffmann et al. (2020) are solely based on nocturnal simulations, while recent studies show the LWP adjustment to be distinct between night- and daytime conditions (e.g. Smalley et al., 2024 and Pugsley et al., 2025). The impact of shortwave heating is not discussed in Glassmeier et al. (2021) and Hoffmann et al. (2020), while we do find it to be yielding a non-monotonic response in LWP over time (cf. Sect. 4.1).

The discussion of time scales is interesting and relevant for the contextualisation of the paper. Thus, a summary of the above paragraph has been added to the discussion section:

This time scale is consistent with the long time scales of around 10 h (Glassmeier et al. (2021)) required for the full LWP adjustment to manifest as based on multiple LES runs of nocturnal stratocumuli. Also the processes identified here, namely longwave cooling and evaporative cooling, which impact entrainment and the response to droplet sedimentation, are consistent with identified leading processes driving these LWP equilibrium states in Hoffmann et al. (2020) and Glassmeier et al. (2021). The equilibrium states themselves are governed by large-scale drivers, such as low-troposphere divergence, surface fluxes, and the background aerosol concentration. The impact of droplet sedimentation may either accelerate or decelerate the rate at which a given equilibrium is approached. We do not quantify this here, as aerosol-cloud interactions and the LWP adjustment are not the focus of this study; instead, our primary objective is to examine the direction of cloud response induced by droplet sedimentation itself. Nonetheless, the impact on adjustment time scales is relevant to explore in future work, as characteristic time scales of changing external parameters and the time scale of LWP adjustments covary along the SCT. The

impacts of which for quantifying the LWP adjustment are discussed in Feingold et al. (2025).

In addition, the diurnal cycle has been shown to drive distinct responses in LWP under day-time and night-time conditions (Smalley et al., 2024; Pugsley et al., 2025). In Sect. 4.1 we also found non-monotonic responses in entrainment speed to droplet sedimentation driven by shortwave heating during the day. This demonstrates the necessity for a more refined analysis of these processes with respect to the diurnal cycle. This was not done here, as our simulation set is too small to stratify for time of day in addition to their position along the SST gradient. While we can stratify for the spatial dimension (i.e. similar conditions in surface forcing), the legs do not coincide in time. For such analysis a much larger set of simulations (or multiple diurnal cycles) would be required.

Minor Comments

Ll. 48 – 51: Is the increase in precipitation just caused by enabling cloud droplet sedimentation and the subsequent vertical redistribution of cloud water?

We agree with the reviewer’s argument that the vertical redistribution leads to a stronger precipitation flux, especially at cloud-base. However, Wyant et al. (2007) to a small extend and Ackerman et al. (2009) to a larger one also show that the surface precipitation rates are increased. So it is not only the vertical redistribution, but also the overall amount of liquid water reaching the surface. That said, to not only focus on the surface precipitation rate, we altered the sentence as follows:

They found that precipitation rates are reinforced at cloud-base as well as the surface in the presence of cloud droplet sedimentation, leading to an overall counteracting effect regarding the stratocumulus to cumulus transition:

Eq. 5: What does the ω' indicate?

We apologise for being unclear here, ω' simply is the correction to the large-scale vertical velocity ω . The prime (analogously for T'_v) denotes the deviation from the reference profile. So after computing the correction ω' through Eq. (5), it is added to ω to account for potential inversion drifts through the large-scale forcings. Thank you for pointing this out, we specified it in the manuscript.

Ll. 166 – 167: What is the “original” vertical velocity?

The “original” vertical velocity refers to the forcings of McGibbon and Bretherton (2017), which we adapted for ICON without adding any WTG correction to it. This is basically the raw large-scale vertical velocity. We agree that this is not fully clear, so we specified it when updating this paragraph. For details, we refer to the point of reviewer #1 regarding Sect. 2.3., where we explain in detail the WTG correction and also present the updated paragraph.

Ll. 242 – 257: I recommend referring to Bohren (1987) here.

We agree with the reviewer that Bohren (1987) is a better reference here. However, we followed the suggestion of reviewer #1 to use the approach of Kurowski et al. (2025) after Meador and Weaver (1980) to include the solar zenith angle in the calculation of the pseudo albedo. Thus, we refer to the comment of reviewer #1 for Sect. 3.1 and the updated manuscript for details.

Ll. 428 – 429: How does evaporative cooling add to longwave cooling? Or do the authors refer to the overall cooling?

We apologise for the lack of clarity. We indeed meant that evaporative cooling and long-wave cooling together increase the overall cooling. We rephrased this as follows:

This re-enables stronger evaporative cooling, which, in combination with the longwave cooling, adds to the total cooling.

Technical Comments

Ll. 42 ff.: Citation style is incorrect.

We thank the reviewer for noting this. We corrected the citation style in this section as well as throughout the whole manuscript where needed.

References

Bohren, C.F., 1987. Multiple scattering of light and some of its observable consequences. *Am. J. Phys*, 55(6), pp.524-533.

Glassmeier, F., Hoffmann, F., Johnson, J. S., Yamaguchi, T., Carslaw, K. S., & Feingold, G. (2021). Aerosol-cloud-climate cooling overestimated by ship-track data. *Science*, 371(6528), 485-489.

Hoffmann, F., Glassmeier, F., Yamaguchi, T., & Feingold, G. (2020). Liquid water path steady states in stratocumulus: Insights from process-level emulation and mixed-layer theory. *Journal of the Atmospheric Sciences*, 77(6), 2203-2215.

Feingold, G., Glassmeier, F., Zhang, J., and Hoffmann, F.: Opinion: Inferring process from snapshots of cloud systems, *Atmos. Chem. Phys.*, 25, 10869–10885, <https://doi.org/10.5194/acp-25-10869-2025>, 2025.

Goren, T., Choudhury, G., Kretzschmar, J., and McCoy, I.: Co-variability drives the inverted-V sensitivity between liquid water path and droplet concentrations, *Atmos. Chem. Phys.*, 25, 3413–3423, <https://doi.org/10.5194/acp-25-3413-2025>, 2025.

Wang, S., Q. Wang, and G. Feingold, 2003: Turbulence, Condensation, and Liquid Water Transport in Numerically Simulated Nonprecipitating Stratocumulus Clouds. *J. Atmos. Sci.*, 60, 262–278, [https://doi.org/10.1175/1520-0469\(2003\)060%3C0262:TCALWT%3E2.0.CO;2](https://doi.org/10.1175/1520-0469(2003)060%3C0262:TCALWT%3E2.0.CO;2).